Biochimica et Biophysica Acta, 590 (1980) 141—158

BBA 47822

A POTENTIOMETRIC AND KINETIC STUDY ON THE RESPIRATORY CHAIN OF FERROUS-IRON-GROWN *THIOBACILLUS FERROOXIDANS*

W. JOHN INGLEDEW * and JOHN G. COBLEY **

Johnson Research Foundation, Department of Biochemistry and Biophysics, University of Pennsylvania, Philadelphia, PA 19104 (U.S.A.)

(Received September 24th, 1979)

Key words: Respiratory chain; ESR; Potentiometry; Cytochrome; Chemolithotrophic bacterium; (T. ferrooxidans)

Summary

The type and number of respiratory chain components present in membranes of *Thiobacillus ferrooxidans* have been investigated. These redox components were resolved potentiometrically and kinetically. Using optical techniques two cytochromes a_1, multiple cytochromes *c* and two cytochromes *b* were detected. By using electron paramagnetic resonance, two copper-containing centres, high and low spin ferric haems and a ferredoxin centre were detected. Based on the combination of a potentiometric resolution and a kinetic study a model for the sequence of the respiratory chain components in the Fe^{2+} to O_2 branch of the *T. ferrooxidans* respiratory chain is proposed.

Introduction

Ferrous iron (Fe^{2+}) can be used by the chemolithotrophic bacterium *Thiobacillus ferrooxidans* as the sole source of energy for growth and CO_2 fixation. Fe^{2+} is oxidised to Fe^{3+} with O_2 acting as the terminal electron acceptor [1]. The bacterium is grown in our laboratory under conditions in which the E_h values of the Fe^{2+}/Fe^{3+} and O_2/H_2O couples are approx. +770 mV and +1100

* Present address: Department of Biochemistry and Microbiology, Irvine Building, North Street, University of St. Andrews, Fife KY16 9AL, U.K.

** Present address: Department of Chemistry, University of San Francisco, San Fransico, CA, U.S.A.

Abbreviations: Hepes, *N*-2-hydroxyethylpiperazine *N*-2-ethane sulphonic acid; EDTA, ethylenediamine tetra-acetic acid; E_h, electrode potential relative to the standard hydrogen half cell; Tes, *N*-tris(hydroxymethyl)methyl-2-aminoethane sulphonic acid; *n*-value, the number of equivalents transferred on oxidation or reduction of a redox component.

mV respectively [2], (the E_m of the O_2/H_2O couple is pH-dependent and the cells are grown at pH 2.0).

The respiratory chain of *T. ferrooxidans* can be considered in two sections: that between Fe^{2+} and O_2 the components of which are present in relatively high concentration and which catalyses the 'downhill' flow of reducing equivalents, and that between Fe^{2+} and the pyridine nucleotide pool which catalyses the 'uphill' electron transport (at the expense of the energy derived from the 'downhill' electron transport) necessary so that CO_2 can be fixed via a Calvin cycle. The respiratory chain components of this latter section are present at relatively low concentrations probably because only one electron moves uphill from Fe^{2+} to pyridine nucleotide for every 20 going downhill to O_2 [3].

We have measured the proton electro-chemical gradient in cells oxidising Fe^{2+} ion [2,4] and obtained a value of about 270 mV in a pH 2.0 medium, this gradient is composed almost entirely of the ΔpH term. So long as the cells remain intact the internal pH is maintained between pH 6.0 and 7.0, and the membrane potential ($\Delta\psi$) is the component which changes in response to the energised state. Thus in studying the respiratory chain components of *T. ferrooxidans* there are three important pH values to be considered: the pH of cell growth which is pH 2.0, the cell matrix pH which is approx. pH 7.0 and the pH optimum for Fe^{2+} oxidation by the membrane preparations which is pH 3.2.

Ingledew et al. [2] have proposed a chemiosmotic model for energy transduction in *T. ferrooxidans* growing on Fe^{2+} oxidation. This model proposes that Fe^{2+} is oxidised externally and e^- are conveyed to the matrix side of the membrane by the respiratory chain where they are consumed with matrix protons in the reduction of O_2 to H_2O. This may be envisaged as two half-reactions separated by a membrane and linked by a chain of redox enzymes:

$$\text{Periplasm}\quad \left.\begin{matrix} 2\,Fe^{2+} \\ 2\,Fe^{3+} \end{matrix}\right) \xrightarrow{2e} \left(\begin{matrix} \tfrac{1}{2}\,O_2 + 2\,H^+ \\ H_2O \end{matrix}\right. \quad \text{Matrix}$$

In the present paper we have investigated further the respiratory chain which links these half-reactions and we also present some information on the 'minor' components which may function between Fe^{2+} and $NAD(P)^+$.

Materials and Methods

Bacterial strain and growth conditions

T. ferrooxidans (strain T.f.3) was obtained from Dr. D. Herbert (Microbiological Research Establishment, Porton Down, Salisbury, Wilts., U.K.) and was grown in a medium containing: $(NH_4)_2SO_4$ (1 mM), KH_2PO_4 (0.2 mM), salts solution (0.2 ml/l), H_2SO_4 (2 ml/l of 98% w/w) and $FeSO_4 \cdot 7\,H_2O$ (180 mM). The components were added in the order listed to a sufficient quantity of distilled water; the pH of the final solution was 2.0 and was not further adjusted. The concentrated salts solution contained: HCl (250 ml/l of 31% w/w), MgO (1.2 M), $CaCO_3$ (10 mM), ZnO (5 mM), $CoCl_2 \cdot 6\,H_2O$ (5 mM), H_3BO_3 (5 mM) and $Na_2MoO_4 \cdot 2\,H_2O$ (5 mM). The growth medium contained

no added copper salt, however copper is present as a contaminant in the $FeSO_4 \cdot 7\ H_2O$ at 0.005%.

Large scale cell growth was achieved in continuous culture in the medium described above. A 60-l polythene aspirator served as the growth vessel (working volume, 50 l). The medium (dilution rate, 0.013 h^{-1}) entered the growth vessel at the top and exited through a nylon tube which extended from the surface of the culture to a collecting reservoir via a port at the base of the aspirator. Air was forced through the growth vessel at a rate of 20 l/min. The culture was maintained at 28° C by means of infra-red lamps, controlled by a thermistor immersed in the culture.

Preparation of electron transport particles

50 l of chemostat effluent was passed through a Sharples centrifuge (25 000 rev./min with a flow rate of 15 l/h) to yield a cell paste of about 3 g wet weight. Electron transport particles were prepared in distilled water at pH 7.0 using a French press as described previously [5] except that the French pressure cell was operated at 16 000 lbs/inch^2, the broken cell suspension was spun twice at 10 000 $\times g$ for 10 min to remove whole cells, and two stages, involving millipore filtration and the addition of $MgSO_4$ (1 mM), were omitted. The supernatant was centrifuged at 100 000 $\times g$ for 1 h to sediment the electron transport particles. The particles were washed once and re-centrifuged.

Redox titrations

For redox titrations the reaction vessels employed were those described by Dutton [6]. In those experiments that were monitored optically, the spectrophotometer used was designed and constructed in the Johnson Foundation. This machine has two monochromators, one of which was set at a fixed reference wavelength and the other was used to scan the sample. The signal obtained from a scan of the fully oxidised material was fed into the memory of a digital computer.

The optical spectra illustrated in this paper are scans from which the fully oxidised spectrum has been subtracted by the computer. The E_h values at which the suspensions were scanned are indicated in the figures.

In redox titrations, to achieve mediation between the platinum electrode and the respiratory chain, the dye systems described by Dutton [6] were suitable and were used at pH 7.0. However at pH 3.2 the only mediator required was 100 μM $FeCl_3$. This Fe^{2+}/Fe^{3+} couple interacted well both with the platinum surface and the respiratory chain, presumably via the Fe^{2+}/Fe^{3+} oxidoreductase. Although the attainment of equilibrium took several minutes after each addition, the oxidation/reduction titrations were reversible. The oxidation/reduction capacities for buffering in the suspension were strong over the entire titration range, probably because of the binding of Fe^{2+} and Fe^{3+} to a variety of sites associated with the membrane preparation. Control titrations were performed in which redox dyes were also present and similar results were obtained (*o*-tolidine, *p*-amino-diethylaniline, Lauth's violet, pyocyanine, indigo trisulphonate and ascorbate). The ferrocyanide-ferricyanide couple was always avoided because of the possible formation of ferrousferricyanide (Prussian blue). Moreover, an oxidant more powerful than ferricyanide was required to

bring about full oxidation of cytochromes a_1 and c. Na_3IrCl_6 proved to be suitable for this purpose, ($IrCl_6^{2-}/IrCl_6^{3-}$ E_m approx. +1.09 V). Although $IrCl_6^{3-}$ absorbs significantly at wavelengths less than 550 nm, on its addition to ETPs * it is immediately reduced to the colourless $IrCl_6^{2-}$. Na_2IrCl_6 was added at the start of the titrations to bring the E_h to approx. +830 mV. At E_h values more positive than +830 mV absorption by $IrCl_6^{2-}$ interfered with cytochrome measurement in the Soret region. Cytochrome reductions were achieved with $FeSO_4$, ascorbic acid or KBH_4. The latter was dissolved in 1 mM potassium phosphate at pH 9.0 and kept on ice. Dithionite proved unsuitable as a reductant as it caused the formation of a black precipitate.

Kinetic analyses

Stopped-flow experiments were conducted in a regenerative stopped-flow apparatus constructed in the Johnson Foundation work-shop [7]. The optical low-temperature kinetics were conducted using a gas flow cooling system attached to either a wavelength-scanning dual-beam spectrophotometer or a fixed wavelength dual-beam spectrophotometer [8,9]. For these experiments electron transport particles were suspended in a buffer containing 10 mM β-alanine sulphate, 40% ethylene glycol (pH 3.0) and 10 mM ascorbate. The suspension was bubbled with carbon monoxide for 5 min. Antifoam was used if necessary. Aliquots of the suspension were transferred to the optical cuvettes and stored at −80°C until needed. Just prior to running a sample at the required temperature the cuvette was transferred to a −20°C bath in the dark and vigorously stirred. This stirring served to introduce oxygen into the suspension. The cuvette was then placed in the spectrophotometer and equilibrated, in the dark, to the required temperature. When this was done the lamp and photomultiplier were switched on and the reaction could then be initiated by flash-photolysis of the oxidase-carbon monoxide compound allowing oxygen present to react.

For the EPR detectable centres kinetics were performed at subzero temperatures after the methods of Strother and Ackerman [10] in aqueous ethylene glycol mixtures. Samples were preincubated at the required temperature, quickly mixed with oxygen, and frozen quickly. All samples for EPR were quickly frozen in an isopentane-cyclohexane freezing mixture (81 K) and samples were then stored in liquid nitrogen until assayed.

All EPR spectra were obtained on a Varian E4 EPR spectrometer (Varian Associates). Temperature control was achieved by a variable temperature cryostat (Air Products Model LTD-3-110). The temperature of the sample was measured by a carbon resistor placed immediately below the sample tube. Quartz glass EPR sample tubes (approx. 3-mm internal diameter) were calibrated with a standard copper sulphate-EDTA solution and values for signal heights were corrected correspondingly.

All standard chemicals used were analytical grade or equivalent and obtained through J.T. Baker Company (New Jersey). The pH buffers and other 'biological chemicals' were obtained through Sigma.

---

* Electron transport particles.

Results and Discussion

Oxidation-reduction titrations of the cytochromes

Fig. 1 shows the results of typical redox titrations performed at pH 3.2 in the alpha band and Soret band spectral regions. In Fig. 1a the cytochrome a_1 absorption (595 minus 575 nm) and the cytochrome c absorption (550 minus 535 nm) are plotted as a function of E_h.

In the case of the 595-575 nm pair a broad absorption change, not due to cytochrome a_1, interferes at E_h values lower than 600 mV. This broad absorption is discussed later (see Fig. 2a). Two independent cytochromes seem to contribute at 595 nm, these have mid-point potentials of +725 mV and +610 mV with n-values of 1.

The redox titrations of the c-type cytochromes (550-535 nm) indicate the presence of more than one species but the mid-point potentials are too close to allow the observation of clear-cut inflection points (Fig. 1). However, our data are consistent with the view of Tikhonova et al. [11], based on liquid N_2 temperature spectra, that two c-type and one c_1-type cytochromes are present.

Since attempts at characterising the cytochromes in the alpha region have indicated complexity, but did not give good resolution, titrations were also conducted in the Soret spectral region. Titration of a_1-type cytochrome bands (Fig. 1b) confirmed the presence of two cytochromes a_1 (E_m (pH 3.2) values of +725 and +610 mV) and also indicated the presence of two additional components (E_m (pH 3.2) values of +280 and +150 mV). These two components were only reduced at E_h values lower than those required to reduce all the other cytochromes and since both exhibited peaks in the difference spectra at

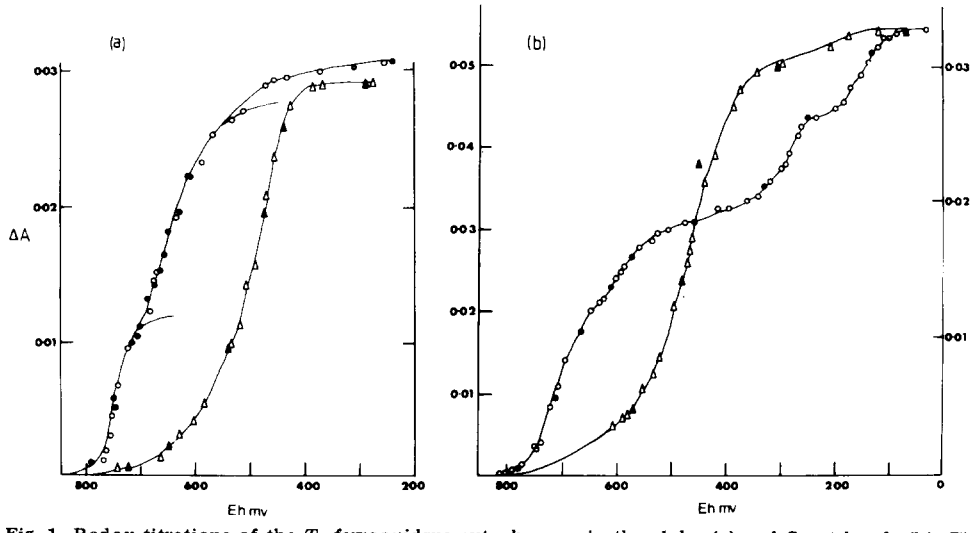

Fig. 1. Redox titrations of the *T. ferrooxidans* cytochromes in the alpha (a) and Soret bands (b). Titrations were performed as described in the Methods section in a medium of 100 mM β-alanine sulphate, pH 3.2. Open symbols denoted reductive titration, closed symbols oxidative titration. (a) The results for the wavelength pairs 595-575 nm (circles) and 550-535 nm (triangles) are shown. The protein concentration was 1.5 mg/ml. (b) The results for the wavelength pairs 440-470 nm (circles, axis on the left) and 418-470 nm (triangles axis on the right) are shown. The protein concentration was 1.0 mg/ml.

a wavelength of about 433 nm it is concluded that these are *b*-type cytochromes.

Titrations of the cytochrome *c* band in the Soret region gave no better resolution than that obtained in the alpha region.

Redox titrations on rusticyanin

Rusticyanin is a 'blue' copper containing protein which is associated with *T. ferrooxidans* electron transport particles which retain their Fe^{2+} oxidising ability [12]. Rusticyanin, in its oxidised form, has a broad absorption band in the blue with an absorption maxima at about 590 nm. The wavelength pair 615-655 nm was chosen to monitor the redox state of this copper centre as at these wavelengths there is no significant interference from cytochromes (cytochrome a_1 has a relatively sharp peak at 597 nm). In Fig. 2a the spectral changes which occur at these wavelengths during a redox titration are illustrated. In the spectra shown in Fig. 2a 575 nm was used as the reference wavelength (hence there can be no differences between spectra at that wavelength); the relatively sharp peak at 597 nm is due to cytochrome a_1, the broader changes most pronounced at 655 nm are largely due to rusticyanin. It should be noted that as the reference wavelength for the spectra (575 nm) is fairly close to that of maximum absorption for the oxidised form of rusticyanin, reduction of the copper is recorded as an increase in absorption at

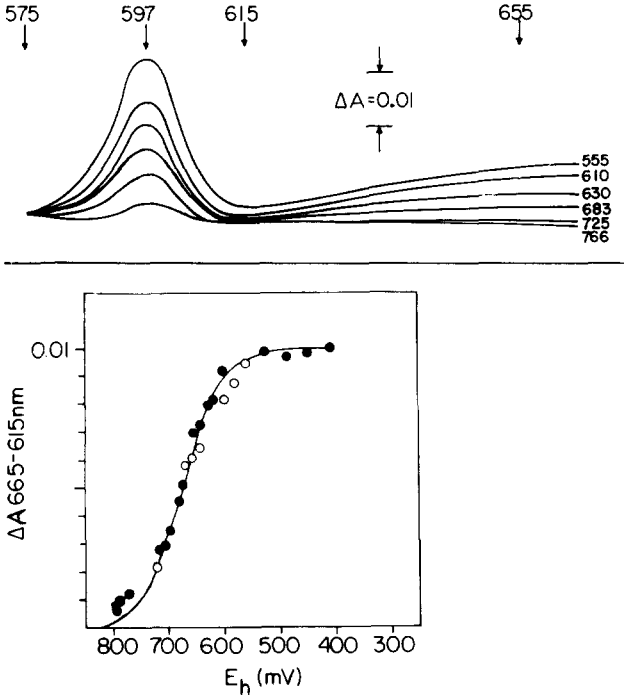

Fig. 2. Redox titration of the broad blue absorption bands. (a) Wavelengths scans at different redox potentials. The baseline is taken at +800 mV and the reference wavelength set at 575 nm. Experimental conditions as for Fig. 1. (b) A plot of absorption difference (665-615 nm) against redox potential. Closed circles reductive titration, open circles oxidative titration.

655 nm in these spectra. In Fig. 2b a typical oxidation/reduction titration is illustrated, a theoretical $n = 1$ curve is drawn. From the spectra it can be seen that at E_h values greater than +600 mV the ratio of absorption at 655 nm to that at 615 is high but at E_h values less than +600 mV the ratio of absorption at 655 nm to 615 is much lower. Two spectral components therefore appear to be present but as the lower potential component appears to change absorbance equally at 615 nm and 655 nm (i.e. it has approximately the same extinction coefficient at these two wavelengths) it will not be apparent in Fig. 2b where the difference of these two wavelengths is plotted. The spectrum of the higher potential component corresponds, spectrally, to rusticyanin [12] and we therefore conclude that the E_m (pH 3.2) value for the Cu^{2+}/Cu^{+} couple of rusticyanin is approx. +680 mV. The spectrally overlapping species with the lower mid-point potential has an even broader absorption peak in the blue than rusticyanin. It is probably this second component which contributed to the redox titration of the cytochromes a_1 (see Fig. 1a) at lower potentials in the α-region; this absorption may be due to a ferric iron chelate [13].

Components of the T. ferrooxidans respiratory chain detected by EPR spectroscopy

Oxidised electron transport particles exhibit a very broad EPR signal which masks the signals of other centres. This signal is temperature-insensitive (Fig. 3) and appears to be due to chelated Fe^{3+}. The signal is abolished by washing the particles several times with buffer containing 50 mM EDTA (pH 7.0) before final resuspension at pH 3.2. Also the signal is not observed in electron transport particles suspended at pH 7.0. The temperature independence of the EPR signal suggests the presence of bound polynuclear Fe^{3+} similar to that found in phosvitin-type proteins (see Ref. 13). On reduction with ascorbate the broad signal disappeared, the redox behaviour of the signal indicated that it is due to multiple centres titrating between +500 mV and +150 mV. The loss of the signal on adjusting the pH to 7.0 may be due to OH^- complexing with the Fe^{3+}, thus altering the properties of the chelate.

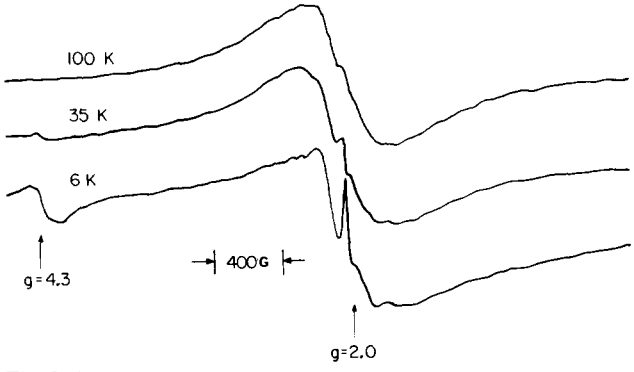

Fig. 3. Ferric ion complex. EPR spectrum of oxidised electron transport particles at different temperatures showing the phosvitin-like EPR absorbance. Field modulation frequency, 100 kHz; microwave power 5 mW; microwave frequency 9.14 GHz; modulation amplitude 20 gauss; scan rate 500 gauss/min; time constant 0.35. The electron transport particles, 10 mg protein/ml were suspended in 100 mM β-alanine sulphate buffer, pH 3.2.

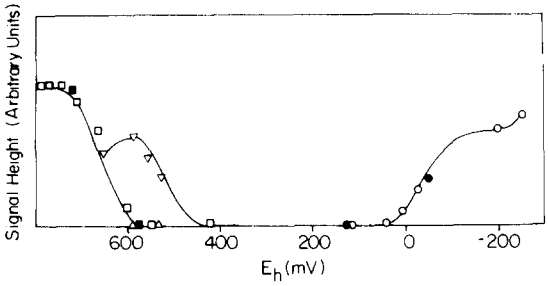

Fig. 4. Redox titrations of EPR detectable components. The signal heights of various EPR absorbances detected in EDTA treated particles are plotted as a function of ambient redox potential at pH 3.2 using the redox dye system. Solid symbols represent oxidative titrations, open symbols reductive titrations. ○———○, g = 1.94; □———□, rusticyanin Cu(II); △———△, second Cu(II).

Examination of the EPR spectra of the EDTA-treated electron transport particles reveals the presence of both high- and low-spin ferric haems, copper centres and (in the reduced samples) ferredoxins. The results of redox titrations of these centres are shown in Fig. 4. These results confirm the value of +680 mV for the E_m (pH 3.2) of rusticyanin obtained spectroscopically and also indicate the presence of a second copper protein, this centre is present in lower concentrations than rusticyanin and has a different EPR line shape (Fig. 5c). This second copper centre has an apparent E_m 3.2 of +520 mV. The (g = 1.94) ferredoxin-type absorption observed in the reduced state titrates with a mid-point potential (pH 3.2) of approximately −50 mV (Figs. 4 and 5d). Two low-spin ferric haem signals are observed, at g = 3.0 and g = 3.33. The signal at g = 3.0 titrates biphasically, the lower potential component having an E_m indicating it originated from a cytochrome c and the higher potential component from cytochrome a_1. Shown in Fig. 5a is an EPR spectrum of the low-spin ferric haem region. The absorption at g = 3.33 titrating in the same potential region as the c-type cytochromes is possibly more akin to a c_1-cytochrome as a g = 3.33 signal is a property of c_1 cytochromes [9].

An EPR spectrum of the high-spin (g = 6.0) region is shown in Fig. 5b. This sample is poised at an intermediate redox potential. At high redox potentials the signal is reversibly lost in a manner that correlated with an increase in the g = 3.0 signal. Lowering the redox potential also causes loss of the high-spin signal.

Redox titrations at pH 7.0

Redox titrations were performed at pH 7.0 in a similar way to those at pH 3.2 described in the preceding sections, although different mediator systems were used. The results of these redox titrations are shown in Fig. 6. Mid-point potentials of approximately +420 mV and +500 mV were determined for the two cytochromes a_1. In Fig. 6a data obtained from redox titrations in the Soret spectral region are shown, the plot for 440 nm (●———●) represents the changes in cytochrome a_1 absorption with small overlapping contributions from cytochromes b at lower potentials. The change in absorbance at 450 nm (□———□) is also shown, the major contributor at this wavelength is cytochrome a_1 with little overlap from b-cytochromes expected. At pH 7.0 80%

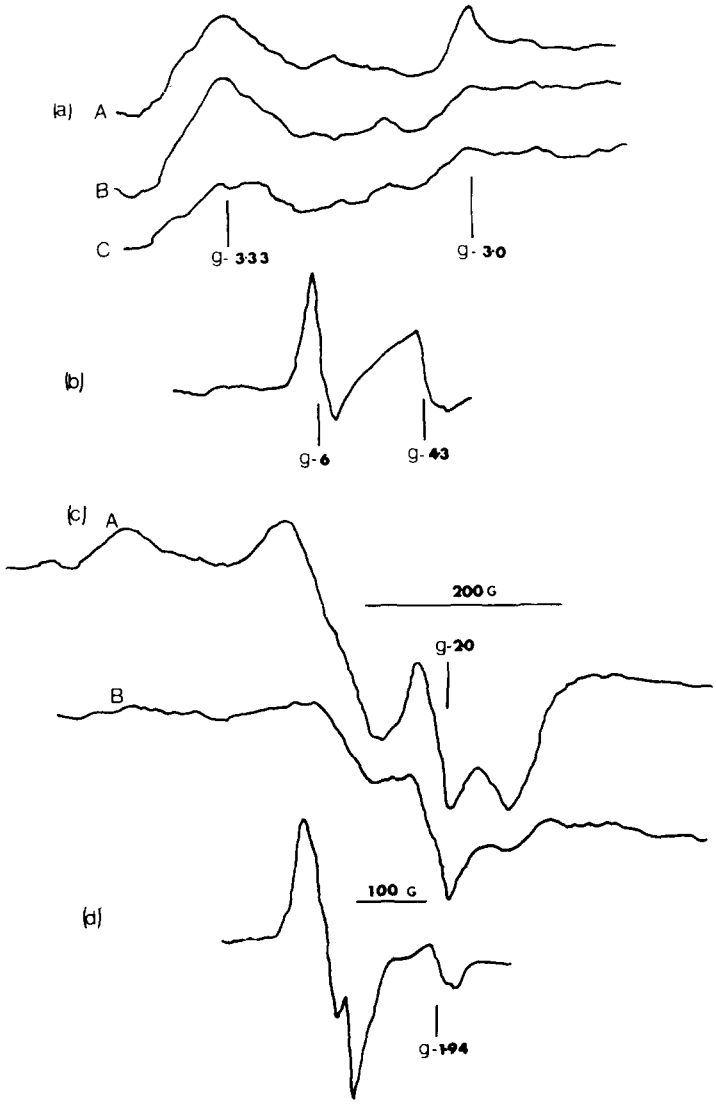

Fig. 5. EPR spectra of *T. ferrooxidans* electron transport particles. (a) EPR spectra of g_z peak of low-spin cytochromes. The electron transport particles were poised at redox potentials of A + 550 mV, B + 505 mV and C + 400 mV (pH 3.2). (b) EPR spectrum of high-spin haem signal. The sample is poised at a redox potential of +600 mV. (c) EPR spectra of the $g = 2.0$ region showing the presence of cupric centres. The samples were poised at A +700, B +550 mV. (d) EPR spectra showing the g_x, g_y absorbance of a ferredoxin-type centre. The sample was dithionite reduced. Electron transport particles (10 mg/protein/ml) were suspended in 100 mM β-alanine sulphate buffer, pH 3.2. The EPR conditions were (a) modulation amplitude 25 G, microwave power 10 mW, temperature 9 K; (b) modulation amplitude 12.5 G, microwave power 10 mW, time constant 1 s, temperature 7 K; (c) modulation amplitude 12.5 G, microwave power 10 mW, temperature 46 K. The microwave frequency was 9.14 GHz and the modulation frequency 100 kHz throughout.

of the cytochrome *c* content of the sub-cellular preparation titrates between 200 and 400 mV but the remaining 20% has an apparent mid-point potential of +500 mV. The EPR detectable centres were also titrated at pH 7.0 (Fig. 6b and c). A mid-point potential of +230 mV for a copper centre was determined

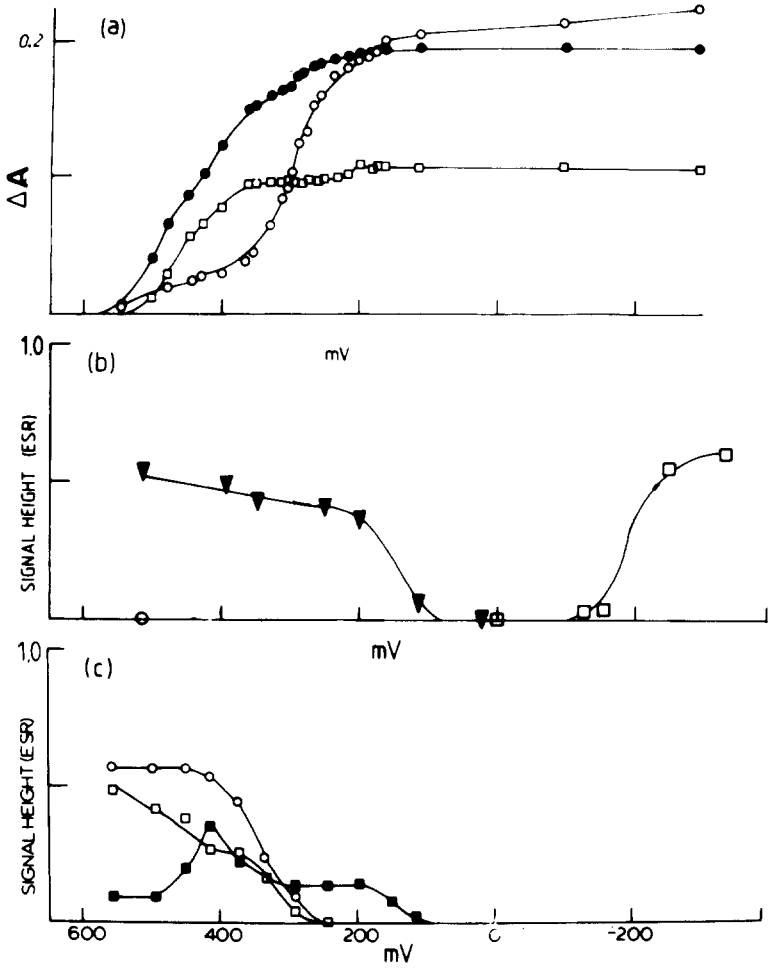

Fig. 6. Redox titrations of *T. ferrooxidans* respiratory chain components at pH 7.0. (a) Optical titrations of the cytochromes. Absorbance differences at 440-470 nm (●———●), 450-470 nm (□———□) and 418-470 nm (○———○) are plotted as a function of redox potential. Experiments were conducted in 50 mM TES buffer, pH 7.0. The redox mediators used were 2-hydroxy-1,4-naphthoquinone 35 μM, duroquinone 20 μM, *N*-methylphenazonium methosulphate 20 μM, diamino durol 30 μM, *N,N,N',N*-tetramethylphenylenediamine 10 μM; σ-tolidine was used with Na_3IrCl_6 as oxidant, ascorbate and dithionite were reductants. EDTA-washed particles were 4.2 mg protein/ml. (b) Titrations of Cu^{2+} and ferredoxin centres. Experimental conditions are as in (a) except that the protein concentration is 10 mg/ml. ▼———▼, $g = 2.07$ (Cu^{2+}); □———□, $g = 1.94$. (c) Titration of high- and low-spin haem signals. Redox titrations performed as for (b): EPR conditions as for Fig. 5 (for low-spin and high-spin respectively). EDTA-washed electron transport particles were used. □———□, $g = 3.0$; ○———○, $g = 3.3$; ■———■, $g = 6.0$ (high spin).

and the $g = 1.94$ signal titrated in the region of −240 mV. This copper centre appears to be similar to the minor copper centre of the pH 3.2 redox titrations. The EPR signal is unlikely to have any contribution from rusticyanin as it is known that rusticyanin is always reduced (by H_2O?) at pH 7.0 (Cobley, J.G., unpublished observations). The very broad EPR signal (Fig. 3) is also absent at pH 7.0.

The results of redox titrations on the EPR signals of the cytochromes are

shown in Fig. 6c, unfortunately, from a comparison of Fig. 6a (the cytochromes measured optically) and Fig. 6c it is not possible to unequivocally state which cytochrome corresponds to which EPR signal. However, by analogy to mammalian systems [14] it could be that the loss of the $g = 3.0$ (higher potential component) and concomitant rise of the $g = 6.0$ signal corresponds to the reduction of the higher potential cytochrome a_1 which would then behave similarly to cytochrome a_3 of mammalian cytochrome oxidase. If this were the case then the reduction of the lower potential cytochrome a_1 would manifest as a loss of high spin ($g = 6.0$) signal. The remaining $g = 3.0$ signal (□———□) and all of the $g = 3.3$ signal (○———○) would then correspond to cytochrome c and c_1 possibly with some contribution from cytochrome b.

Kinetics of oxidation of redox components studied at different temperatures

The foregoing part of this paper was concerned with the analysis of the types, number and mid-point potentials of the redox components present in *T. ferrooxidans* membrane preparations. In this present section we use kinetic methods in an attempt to ascertain the sequence in which the respiratory components function. To assist in determining the sequence of the components the kinetics have been studied at different temperatures (23° C, −20° C and −33° C) and states (aqueous, aqueous-ethylene glycol slurry, solid) as some steps proved to be more temperature-sensitive than others.

At 23° C a recycling stopped-flow apparatus was used in combination with a spectrophotometer to determine the time course of cytochrome oxidation subsequent to O_2 addition. Prior to the mixing of O_2 (15 nmol O_2 per ml) the membrane preparation was reduced by ascorbate.

In Fig. 7a typical cytochrome oxidation traces are shown, the upper trace shows cytochrome a_1 oxidation (Soret region) and the lower trace cytochrome c oxidation (alpha band). Analysis of such oxidation time courses (Fig. 7b) shows that there are, at least, two components contributing in both the a_1 and c oxidations. The semi-logarithmic plots (Fig. 7b) indicate that the oxidations are first order and give half-times for the oxidation of c-type cytochromes of 50 ms and 150 ms. The oxidation of the a_1-type cytochromes is more complex, the first phase of oxidation is apparently first order with a half-time for oxidation of 20 ms but this phase is followed by a lag of about 250 ms before the onset of a second phase of oxidation, this latter phase has a half-time of about 100 ms. A kinetic profile of the Soret region is shown in Fig. 8, no spectral anisotropy can be detected for either cytochromes a_1 or c either in this spectrum or in their alpha-bands. Fig. 8 indicates that there is no detectable spectral difference, other than extent of absorption change, after the first cytochrome a_1 and c have been oxidised and full oxidation. However in the case of cytochrome a_1 it is known from potentiometric analysis that there are two components and that the higher potential component accounts for 60% of the absorption change in the Soret region and the lower potential component only 40%. This situation is reversed in the analysis of the alpha-band (Fig. 1a and b). The kinetics of cytochrome oxidation in the Soret band indicate that approximately 60% of the cytochrome a_1 content is oxidised in the first phase, suggesting perhaps, that the first component to be oxidised is the higher potential cytochrome a_1.

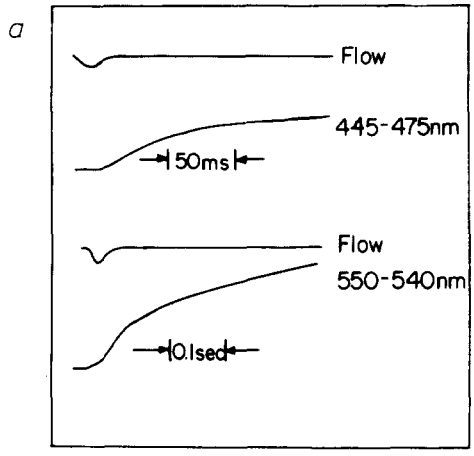

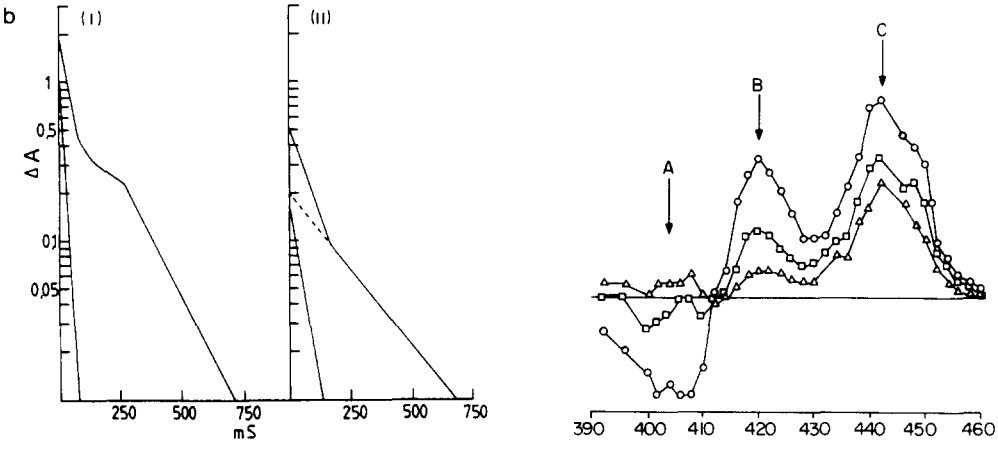

Fig. 7. Stopped-flow kinetics of cytochrome oxidation. (a) The rapid phase of cytochrome $a1$ (top) and c (bottom) oxidation are shown. (550-540 nm cytochrome c; 445-475 nm cytochrome a_1). Electron transport particles (to 2.1 mg protein/ml) were suspended in buffer containing 50 mM β-alanine sulphate and 5 mM ascorbate, pH 3.2. The total volume in the main syringe was 14 ml. (b). Semilogarithmic plots of the time course of cytochrome oxidation obtained using the stopped-flow. Plots are derived from traces similar to those shown in Fig. 2. (I) Cytochrome a_1. The upper trace shows the overall process, the lower, the projected behaviour of the faster component. (II) Cytochrome c, the upper trace shows the overall change, the lower trace the faster component alone (assuming first-order kinetics).

Fig. 8. Kinetic profile of the Soret region. The points are taken from experiments performed over the wavelength range (reference wavelength 475 nm). The change in absorbance after 50 ms (△———△), 100 ms (□———□) and 1.6 s (○———○) is shown. Experimental conditions are the same as in Fig. 7, and described in Methods.

Although the room temperature kinetics demonstrated that one of the a_1-type cytochromes was the first detectable component oxidised it did not resolve the sequence of the slower a_1 component ($t_{1/2}$ 100 ms after 250 ms lag) and the two c-type cytochromes ($t_{1/2}$ 50 ms and 150 ms). To help resolve these problems a further kinetic analysis was carried out, this time at temperatures below 0°C where the reactions will be slowed down. In these studies

of kinetics at low temperature the oxidation reaction was initiated by flash photolysis of the oxidase-CO compound in the presence of O_2 which can then react with the oxidase.

Spectra taken by a scanning dual-beam spectrophotometer at different time intervals after flash-photolysis of the oxidase-carbon monoxide compound of the oxidase in preparations suspended at −20°C (30% ethylene glycol) are shown in Fig. 9a. All the a_1 and c cytochrome undergoes oxidation. The cytochrome a_1 goes fully oxidised more rapidly than the instrument resolution time. Cytochrome c oxidation may be biphasic as shown by points taken from spectra, such as those in Fig. 9b. The cytochrome c oxidation can probably be split into a 'fast' component and a slower component with a $t_{1/2}$ of approx. 20 s. The numerals I and II in Fig. 9b indicate the time spans of the spectra presented in Fig. 9a.

The spectrophotometric studies at −20°C were supplemented by EPR studies, the results of which are shown in Fig. 9c. The appearance of a Cu^{2+} signal (△———△) is plotted as a function of time after flash initiation of oxidation; the samples were quenched for EPR studies by plunging into a hexane/isopentane freezing mixture cooled to near 77 K. At −20°C the oxidation of the copper has a $t_{1/2}$ of approx. 12 s. Also shown in Fig. 9c is the rise of the $g = 4.3$ signal (△———△). The $g = 4.3$ signal comes from tetrahedral Fe^{3+} and it is presumably generated through respiratory oxidation of residual Fe^{2+}. The $t_{1/2}$ for the rise of the $g = 4.3$ signal is about 22 s, however, no estimate of its (spin) concentration could be made.

At −20°C the aqueous-ethylene glycol buffer used is a slurry and to see if more information which would assist in determining the sequence of the components could be obtained from studying kinetics on the solid state the temperature was lowered to −33°C.

The progress curves of cytochrome oxidation following flash dissociation of the oxidase-CO compound at −33°C are shown in Fig. 10. The cytochrome c is oxidised monophasically with a $t_{1/2}$ of about 15 s and is re-reduced in minutes, only about a third of the cytochrome c pool is apparently being turned over. All of the cytochrome a_1 is oxidised rapidly ($t_{1/2}$ 2 s). A significant artifact due to the dissociation of the oxidase-CO compound is not expected as there is no significant absorbance change due to CO in the a_1 α-band. It appears that at this temperature only one c-type cytochrome is oxidised, the other c-type cytochromes (and rusticyanin) are 'frozen' out. These observations may be explained if the oxidation of these latter c-cytochromes and rusticyanin require diffusional mobility in the aqueous phase, this cannot occur in the solid state where only those molecules of c proximal to the oxidase can be oxidised.

Table I shows the half-time of oxidation, first order rate constant and electron transfer rate for the different kinetic components. Under the same experimental conditions (pH 3.0, 23°C) the maximal rate of Fe^{2+} oxidation by electron transport particles corresponds to approx. 10 nmol e^-/s per mg protein. The concentration of cytochromes a_1 in the preparation was estimated to be approx. 3.0 nmol/mg protein. Although there is some variability between preparations in the cytochrome a_1 content, nonetheless these values are high, the haem a content being, on average, about twice that of ox heart sub-mitochondrial particles. Tikhonova et al. [11] reported values of 1.4 nmol mg/

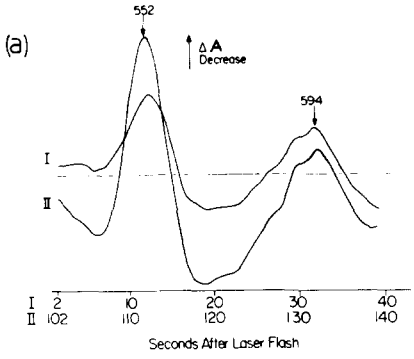

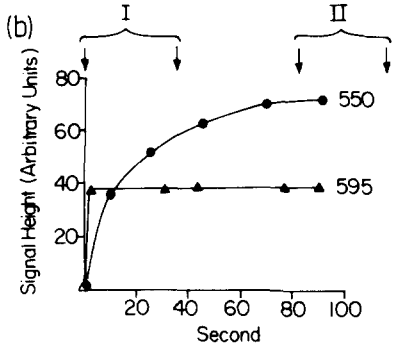

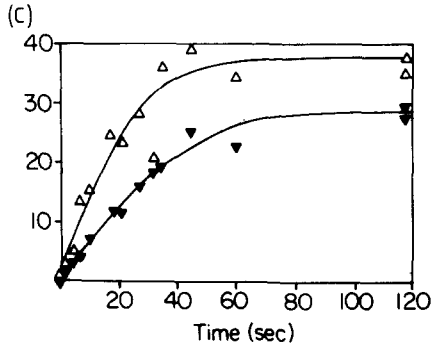

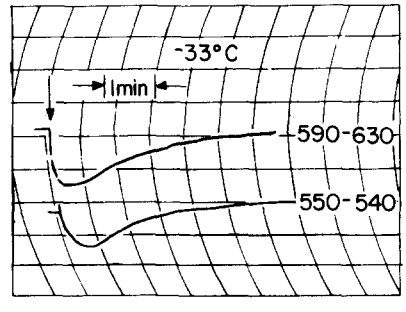

Fig. 9. Oxidation kinetics at −20°C. (a) Spectra taken at different intervals after initiation of oxidation by laser flash at −20°C. Electron transport particles (9 mg protein/ml) were suspended in 10 mM ascorbate/50 mM β-alanine sulphate/30% ethylene glycol buffer, pH 3.2. The suspension was saturated with CO, O_2 was stirred in at −20°C, in the dark, prior to flash dissociation of the CO compound. Note that the reaction is progressing as the spectrum is being run. (b) Progress curve of cytochrome oxidation at −20°C. The experimental conditions were as for Fig. 5. The points were taken from a series of spectra. The ranges denoted, I and II are those covered in the spectra of (a). (c) Oxidation of Cu^+ and Fe^{2+} at −20°C. Samples were prepared as described in Methods; being stored at 77 K while awaiting measurement by EPR. △———△, g = 2.03 (Cu^{2+}); ▼———▼, g = 4.3 (Fe^{3+}). Conditions were as for Fig. 5. EPR spectra were taken at 30 K.

Fig. 10. Kinetics of oxidation of cytochrome a_1 and c at −33°C. Experiments were conducted as in Fig. 9a, b, except for the different temperature and the use of a fixed wavelength pair.

TABLE I

SUMMARY OF THE PSEUDO-FIRST ORDER RATE CONSTANTS FOR CYTOCHROME OXIDATION AND MAXIMAL ELECTRON-TRANSFER RATES CALCULATED FROM THE RATE CONSTANTS AND CYTOCHROME CONCENTRATION

The pseudo-first order rate constants (K) were calculated from the half times of oxidation. Maximal rates of electron transfer (as nequiv. s per mg protein) were calculated as the product of the pseudo-first order rate constant for a particular cytochrome and the concentration (nmol/mg protein of that component determined from the spectrometric recording of its oxidation). The maximal observed electron-transfer rate, oxidation of Fe^{2+}, at pH 3.0 and 23°C was 10 nmol/s per mg protein.

Cytochrome	Temperature (°C)	$t_{1/2}$ (s)	K (s^{-1})	nmol e/s per mg protein
c	23	0.150	4.62	9.9
c	23	0.50	13.86	29.7
a_1	23	0.100	6.13	10.4
a_1	23	0.020	34.6	51.9
c	−36	5	0.138	0.21
(a_1a_1)	−36	2	0.346	0.52

protein cytochrome c and 1.06 nmol/mg protein for whole cells of *T. ferrooxidans*.

Cobley and Haddock [12] have shown that the kinetics of both cytochrome c and a_1 reduction to steady-state levels by addition of Fe^{2+} are biphasic. The apparent $t_{½}$ values being 3 ms and 25 ms for cytochrome c and 75 ms and 15 s for cytochrome a_1. This implies that the site of Fe^{2+} oxidation is closer to the c-cytochrome than to the a_1-cytochrome. There is also the implication that one of the a_1-cytochromes is not on the main respiratory pathway as its rate of reduction is apparently too slow. Alternatively the slow reduction of one of the a_1 components may be due to secondary effects on a multicentre (e.g. both a_1 haems and copper centres) enzyme complex, or in this latter case, anaerobiosis.

In our work with *T. ferrooxidans* there are three important pH values. These are the pH of growth (pH 2), the pH optimum for Fe^{2+} oxidation in subcellular preparations (pH 3.2) and the internal, cytosolic pH, during growth, which is in the region of neutrality [2,3]. Physiologically it is apparent that for growing cells the intracellular and extracellular pH are important and the functional mid-point potential of any given respiratory chain component will depend upon with which phase it tends to equilibrate.

Fig. 11 summarizes the type, number and mid-point potentials of the *T. ferrooxidans* respiratory chain redox components. The mid-point potentials are shown as determined at pH 3.2 and pH 7.0 and it is clear that most of the components have pH-dependent mid-point potentials; the only exception to this may be rusticyanin as it was not possible to obtain a mid-point potential value for this component at pH 7. Rusticyanin is always reduced at pH 7 when in equilibrium with the buffering system.

The a_1-type cytochromes present in *T. ferrooxidans* have mid-point potentials of +725 mV and +610 mV at pH 3.2 and +500 mV and +420 mV at pH 7.0.

Cytochrome a_1 has been studied by potentiometric techniques in two other systems, *Nitrobacter* and *Escherichia coli*; in both systems the cytochrome a_1

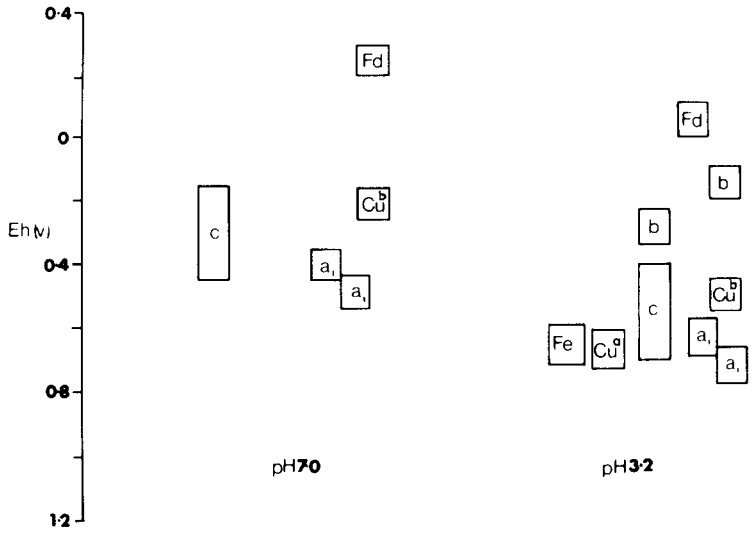

Fig. 11. Thermodynamic profile of the redox centres of *T. ferrooxidans* at pH 7.0 and 3.2. The position of the centre on the redox potential axis denotes the approximate mid-point potential of the component. Fd, ferredoxin; *a*, *b* and *c*, types of cytochrome; Cu^a, rusticyanin; Cu^b, second copper centre.

content is also composed of two approximately equal components with different mid-point potentials. The seemingly obligatory presence of two haem *a*-cytochromes may be related to function as it is in mammalian cytochrome aa_3.

Potentiometrically the *c*-type cytochromes are not clearly resolvable. Approximately 20% of the total cytochrome *c* absorption change during a redox titration occurs at a distinctly higher redox potential than the remainder of the change, this is evident at both pH 3.2 (E_m + 650 mV) and pH 7.0 (E_m + 500 mV). At pH 3.2 it is apparent that more than one component contributes to the remaining 80% of the absorption change; this suggests a minimum of three *c*-type ($c + c_1$) cytochromes in this bacterium. Kinetically two cytochrome *c* components are resolved, these are present in approximately equal concentrations and it is likely that the 20% cytochrome *c* component's oxidation is obscured by these larger changes.

A third type of cytochrome, cytochrome *b*, appears to be present in *T. ferroxidans* membranes, the concentration of the *b*-type cytochromes is less than for *c*- and *a*-type cytochromes and the E_m values are lower suggesting a role in the 'up-hill' electron transfer pathway to NAD^+, rather than in the transfer of electrons from Fe^{2+} to O_2. In the present work only spectra of the Soret region indicative of *b*-cytochromes are shown, however, an optical difference spectrum taken at liquid N_2 temperature clearly showing absorbance at 560 nm in *T. ferrooxidans* has been published [11].

T. ferrooxidans contains high concentrations of a 'blue' copper protein. This protein has been partially purified by Cobley and Haddock [12] and others [15] who found that the protein is reducible by Fe^{2+}. We have determined the $E_{m_{3,2}}$ of rusticyanin to be +680 mV. An EPR spectrum of rusticyanin has been published [12] and we observed similar spectra in membrane preparations.

On the basis of our potentiometric and kinetic analysis of the *T. ferro-*

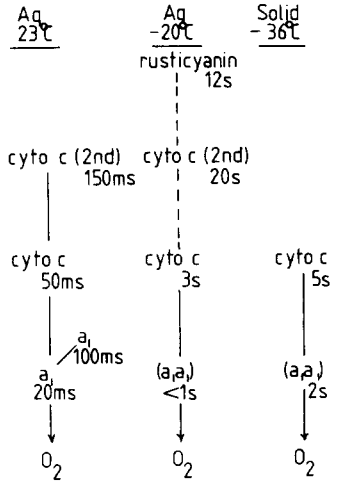

Fig. 12. Summary of $t_{1/2}$ values at three different temperatures, aqueous (Aq) 23°C, −20°C and frozen (solid) −36°C. The order of components, from top to bottom, denotes the suggested sequence.

oxidans respiratory chain components we suggest that their functional sequence is as indicated in Fig. 12. The data on the sequence of the slower *c*-type cytochrome and the copper protein rusticyanin are incomplete; this stems from the difficulty of following the redox state of rusticyanin optically and also quantifying it in different preparations. Nonetheless, rusticyanin has been purified and shown to be directly reducible by Fe^{2+} [12,15]. Thus it is suggested that Fe^{2+} reduces rusticyanin which then reduces a cytochrome *c*, this cytochrome *c* then reduces a second cytochrome *c* which in turn reduces the oxidase.

Virtually nothing is known about the arrangement in the membrane of the respiratory chain component of *T. ferrooxidans*, however, several dispositions can be inferred indirectly. Ingledew et al. [2] have placed the O_2 : reductase reaction in the cellular matrix after studies using azide as an inhibitor. The Fe^{2+} is unlikely to be oxidised inside the cell because above pH 4.0 it is auto-oxidisable and Fe^{3+} is very insoluble as the hydroxide (it is known that the internal pH of *T. ferrooxidans* cells is maintained near neutrality when the external pH is 2.0 [2,4,16]). Also rusticyanin and two *c*-type cytochromes are readily soluble in aqueous buffer (no detergent) suggesting that they are unlikely to dwell in the hydrophobic region of the membrane [12,15,16]. A recent study of the effects of a paramagnetic probe on the EPR properties of rusticyanin in different membrane preparations has led to the conclusion that rusticyanin is located in the periplasmic space [16].

Acknowledgements

We are grateful to Dr. B. Chance for many helpful discussions and financial support and to Dr. B.A. Haddock and Mr. G.A. Reid for helpful criticism of the manuscript.

References

1 Suzuki, I. (1974) Ann. Rev. Microbiol. 28, 85—101
2 Ingledew, W.J., Cox, J.C. and Halling, P.J. (1977) FEMS Lett. 2, 193—197
3 Landesman, J., Duncan, D.W. and Walden, C.C. (1966) Can. J. Microbiol. 12, 25—33
4 Ingledew, W.J., Cox, J.C., Jones, R.W. and Garland, P.B. (1978) in Frontiers of Biological Energetics (Scarpa, A., Dutton, P.L. and Leigh, J.S., eds.), pp. 334—341, Academic Press, New York, NY
5 Bodo, C. and Lundgren, D.G. (1974) Can. J. Microbiol. 20, 1647—1652
6 Dutton, P.L. (1971) Biochim. Biophys. Acta 226, 63—80
7 Chance, B. (1963) in Techniques of Organic Chemistry, Vol. 8, 2nd edn., (Friess, S.L. and Weissberger, A., eds.), pp. 728—735, Interscience Publishers, New York, NY
8 Chance, B. and Graham, N. (1971) Rev. Sci. Instrum. 42, 941—945
9 Chance, B., Graham, N. and Legallais, V. (1975) Anal. Biochem. 67, 552—579
10 Strother, G.K. and Ackerman, E. (1961) Biochim. Biophys. Acta 47, 317—326
11 Tikhonova, G.V., Lisenkova, L.L., Doman, H.G. and Skulachev, V.P. (1967) Biokhimiya 32, 725—734
12 Cobley, J.G. and Haddock, B.A. (1975) FEBS Lett. 60, 29—33
13 Webb, J. (1975) in Techniques and Topics in Bioinorganic Chemistry (McAuliffe, C.A., ed.), pp. 271—306, Halsted
14 Leigh, J.S., Wilson, D.F., Owen, C.S. and King, T.E. (1974) Arch. Biochem. Biophys. 160, 476—486
15 Cox, J.C. and Boxer, D.H. (1978) Biochem. J. 174, 497—502
16 Ingledew, W.J., Angiolillo, P.J., Reid, G.A. and Hoddinott, M.H. (1979) Abstr. 11th International Congress of Biochemistry, Toronto, 06-3-R79, p. 432